Gravity with higher curvature terms

BUM-HOON LEE

SOGANG UNIVERSITY

Sogang University

Contents

1. Motivation :

Why Gauss-Bonnet Term?

Low energy effective theory from string theory
→ Einstein Gravity + higher curvature terms
Gauss-Bonnet term is the simplest leading term.

Q : What is the physical effects of Gauss-Bonnet terms?

1) Effects to the Black Holes.

No-Hair Theorem of Black Holes

Stationary black holes (in 4-dim Einstein Gravity) are completely described by 3 parameters of the Kerr-Newman metric :
mass, charge, and angular momentum (M, Q, J)

Werner Israel(1967), Brandon Carter(1971,1977), David Robinson (1975)

Hairy black hole solution ?
In the dilaton-Gauss-Bonnnet theory → Yes!
Exists the minimum mass of BH
Affects the stability, etc.

2) Effects in the Early Universe.

No-Hair Theorem of Black Holes

Werner Israel(1967),
Brandon Carter(1971,1977),
David Robinson (1975)

Stationary black holes (in 4-dim Einstein Gravity) are completely described by 3 parameters of the Kerr-Newman metric :
mass, charge, and angular momentum (M, Q, J)

- **A rotating black hole (one with angular momentum) has an ergoregion around the outside of the event horizon**
- **In the ergoregion, space and time themselves are dragged along with the rotation of the black hole**

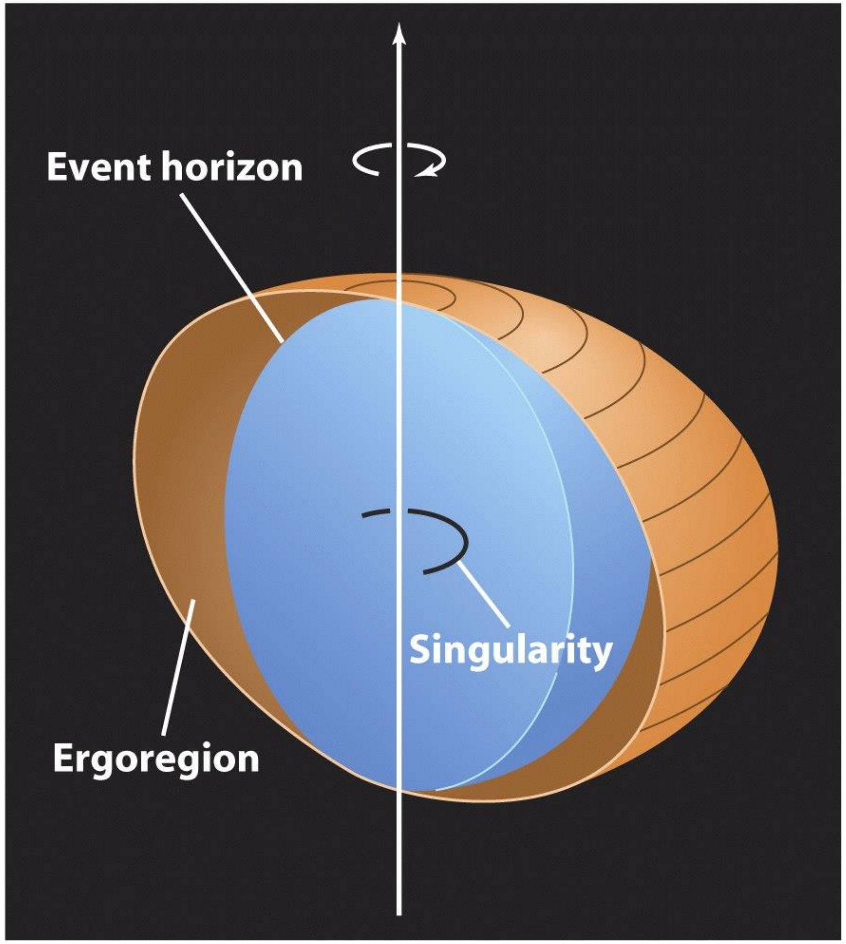

Hairy black hole solution is possible in the dilaton-Gauss-Bonnnet theory.

Colliding Galaxies: A Black Hole Merger

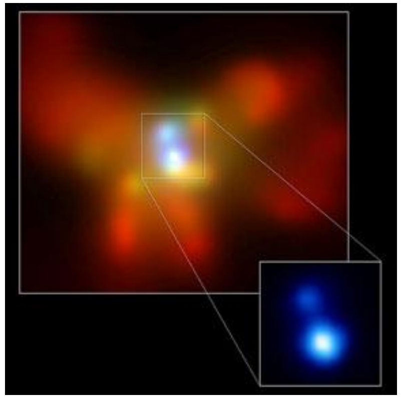

NASA / CXC / MPE / S. Komossa, et al.

Actual observations provide evidence and data for computer simulations. What does it look like when black holes collide?

Colliding Black Holes :
A Black Hole Merger
+ Gravitational Wave

Q: A Black Hole unstable ?
splitting
into two Black Holes ?

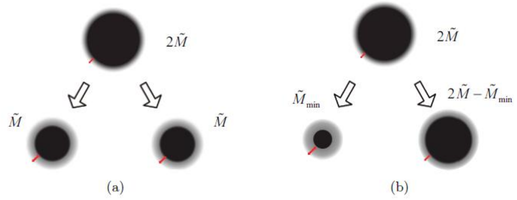

GW150914

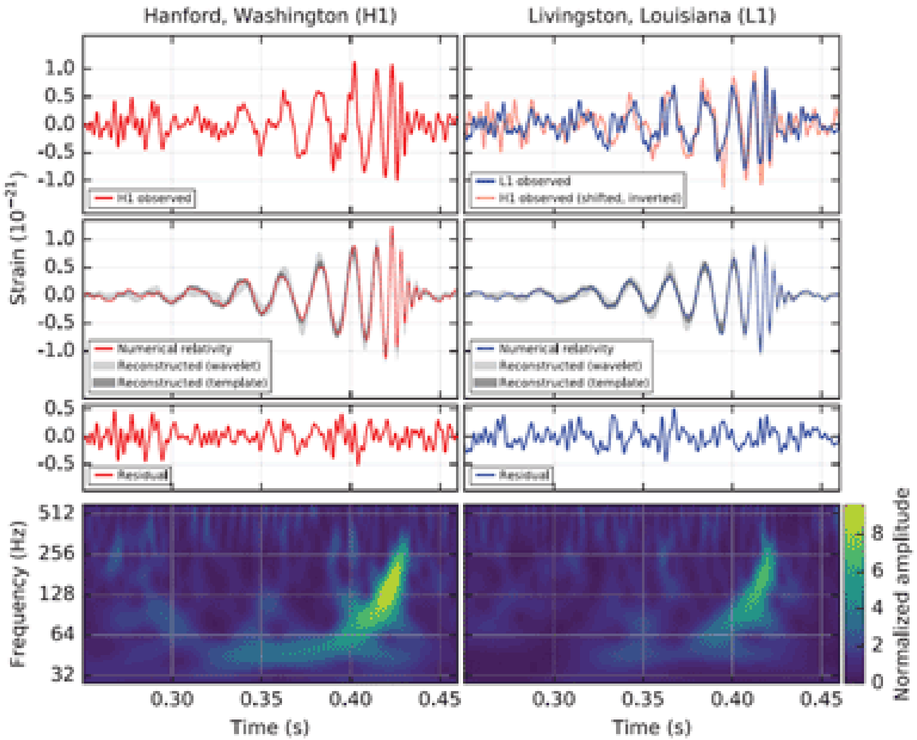

Holography

(asymptotic) AdS Black Hole in d+1 dim

↔

Quantum System in d dim.

Instability of Black Holes

↔ instability of Quantum System

Hence,

instability of AdS BH

↔ phase transitions in Quantum System

* Black holes in higher dimensions are quite diverse !

2. Black Holes in the Dilaton Einstein Gauss-Bonnet (DEGB) theory

W.Ahn, B. Gwak, BHL, W.Lee, Eur.Phys.J.C (2015)

2-1) Einsten Gauss-Bonnet (EGB) theory

Action

$$S = \int d^4x \sqrt{-g}\left[\frac{1}{2\kappa^2} R + \alpha R_{GB}^2 - \frac{1}{2} g^{\mu\nu}\partial_\mu\phi\partial_\nu\phi\right]$$

where $g = \det g_{\mu\nu}$ and $\kappa \equiv 8\pi G$ $R^2_{\rm GB} = R^2 - 4R_{\mu\nu}R^{\mu\nu} + R_{\mu\nu\rho\sigma}R^{\mu\nu\rho\sigma}$

The Gauss-Bonnet term

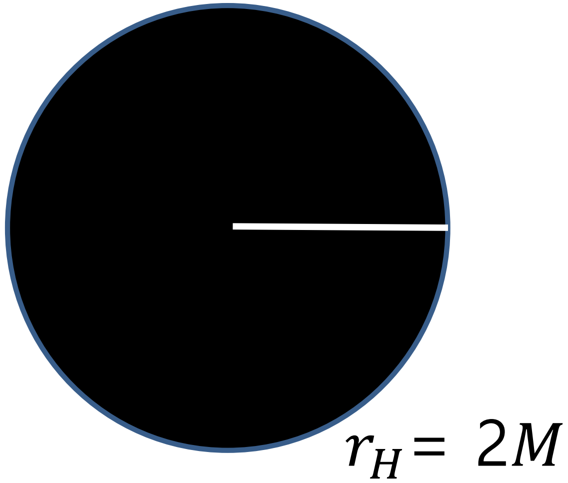

Black Hole solution

$$ds^2 = -\left(1-\frac{2M}{r}\right) dt^2 + \frac{dr^2}{\left(1-\frac{2M}{r}\right)} + r^2 d\Omega^2$$

$\phi = 0$ No hair

Horizon

$r_H = 2M$

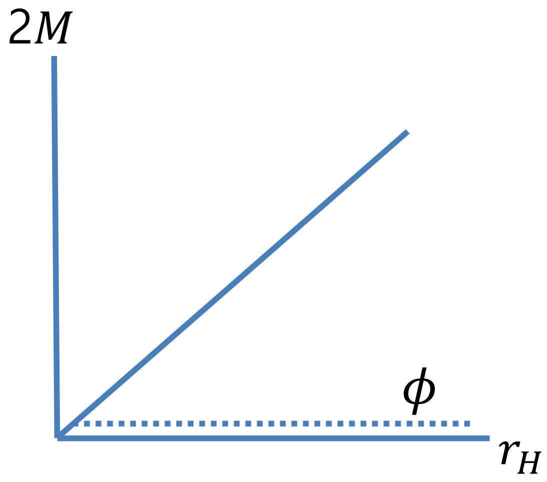

Note :

1) For the coupling α = 0, the theory becomes the Einstein gravity.

2) GB term is a surface term, not affecting the e.o.m. Hence,
The black hole solution is the same as that of the Schwarzschild one.

3) However, the GB term contributes to the black hole entropy and influence stability.

2-2) Dilaton-Einstein-Gauss-Bonnet (DEGB) theory : Hairy black holes

Action

$$I=\int_{\mathcal{M}}\sqrt{-g}d^4x\left[\frac{R}{2\kappa}-\frac{1}{2}\nabla_\alpha\Phi\nabla^\alpha\Phi+\boxed{\alpha e^{-\gamma\Phi}R^2_{\rm GB}}\right]+\oint_{\partial\mathcal{M}}\sqrt{-h}d^3x\frac{K-K_o}{\kappa}, \quad (1)$$

Guo,N.Ohta & T.Torii, Prog.Theor.Phys. 120,581(2008);121 ,253 (2009); N.Ohta &Torii,Prog.Theor.Phys.121,959; 122,1477(2009);124,207 (2010); K.i.Maeda,N.Ohta Y.Sasagawa, PRD80, 104032(2009); 83,044051 (2011) N. Ohta and T. Torii, Phys.Rev. D 88 ,064002 (2013).

where $g=\det g_{\mu\nu}$ and $\kappa\equiv 8\pi G$

The GB term :

$$R^2_{\rm GB}=R^2-4R_{\mu\nu}R^{\mu\nu}+R_{\mu\nu\rho\sigma}R^{\mu\nu\rho\sigma}$$

Note :

1) For $\gamma=0$, DEGB theory becomes the Einstein-Gauss-Bonnet (EGB) theory, with the GB term becoming the boundary term

2) The symmetry under $\gamma\to-\gamma, \Phi\to-\Phi$. allows choosing γ positive without loss of generality.

3) α scaling :The coupling α dependency could be absorbed by the r → $r/\sqrt{\alpha}$ transformation. However, the behaviors for the α = 0 case cannot be generated in this way. Hence, we keep the parameter α, to show a continuous change to α = 0.

The Einstein equations and the scalar field equation are

$$R_{\mu\nu} - \frac{1}{2}g_{\mu\nu}R = \kappa\left(\partial_\mu\Phi\partial_\nu\Phi - \frac{1}{2}g_{\mu\nu}\partial_\rho\Phi\partial^\rho\Phi + T^{GB}_{\mu\nu}\right), \quad (2)$$

$$\frac{1}{\sqrt{-g}}\partial_\mu[\sqrt{-g}g^{\mu\nu}\partial_\nu\Phi] - \alpha\gamma e^{-\gamma\Phi}R^2_{GB} = 0, \quad (3)$$

Note :

1) All the black holes in the DEGB theory with given non-zero couplings α and γ have hairs.
I.e., there does not exist black hole solutions without a hair in DEGB theory.
(If we have Φ = 0, dilaton e.o.m. reduces to R^2_{GB} = 0. so it cannot satisfy the dilaton e.o.m..)

2) Hair Charge Q is not zero, and is not independent charge either.

Coupling γ dependency of the minimum mass for fixed α 1/16.

γ=√2(green),γ=1.3(cyan),γ=1.29(blue)
γ=1/2(red), γ=1/6(black), γ=0(purple)

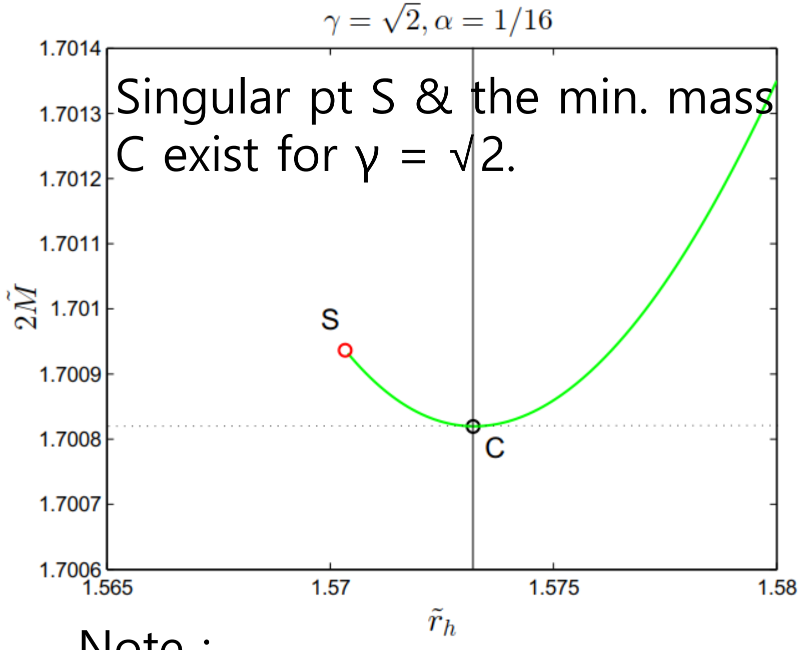

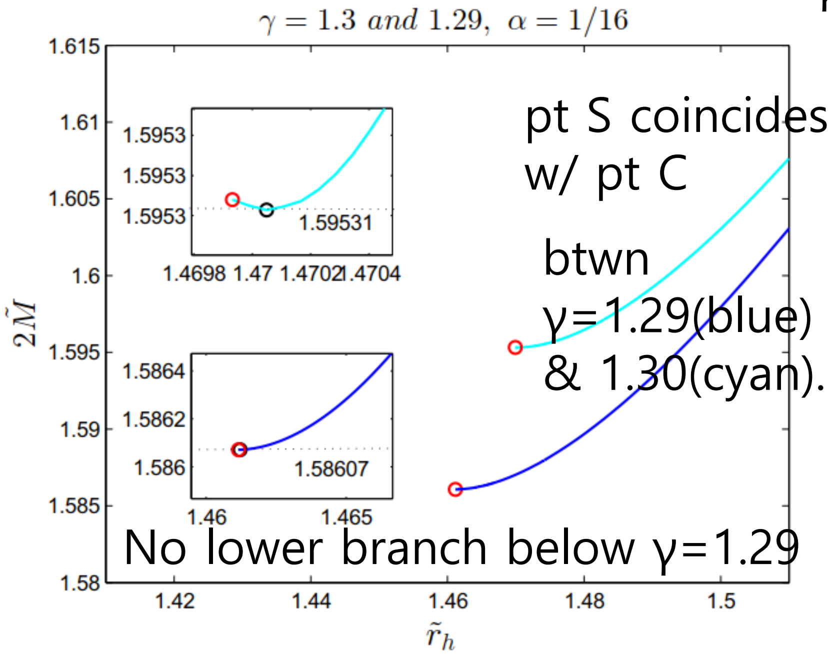

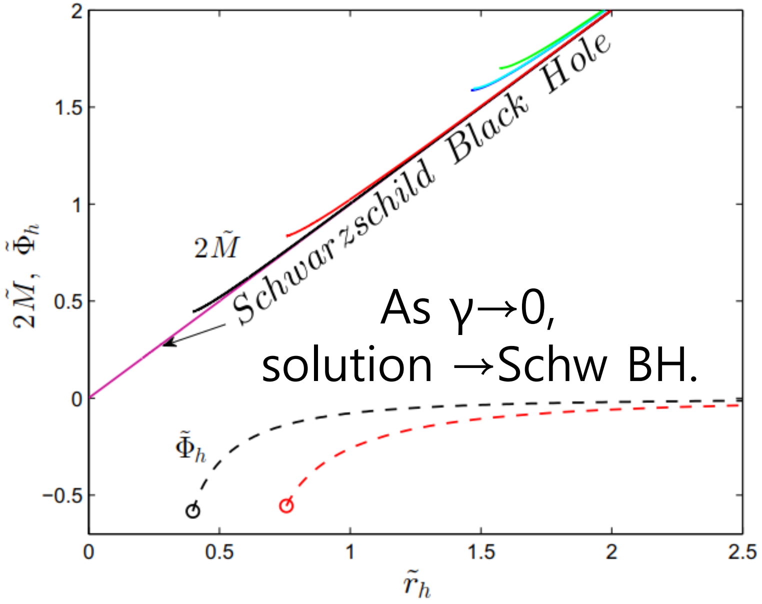

Note :

1. For large γ, sing. pt S & extremal pt C (with minimum mass $\tilde{M}$) exist.
2. The solutions between point S and C are unstable for perturbations and end at the singular point S , I.e., there are two black holes for a given mass in which the smaller one is unstable under perturbations.
3. As γ smaller, the singular point S gets closer to the minimum mass point C.
4. Below γ=1.29, the solutions are perturbatively stable and approach the Schwarzschild black hole in the limit of γ going to zero. These solutions depend on the coupling γ.
5. If DEGB BH horizon becomes larger, the scalar field goes to 0, and the BH becomes a Schwarzschild BH.

GB term → repulsive gravity effects !!!

Q: How about the properties, such as Stability & implication to the cosmology, etc ?

Note : Black Hole Stability

Perturbative Gravitational (in)stability

Perturbations of a black hole space-time

by adding fields or by perturbing the metric.

The typical equations in the linear approximation :

$$-\frac{d^2R}{dr_*^2} + V(r,\omega)R = \omega^2 R,$$

Quasinormal modes :
solutions of the wave equation, satisfying specific boundary conditions at the black hole horizon and far from the black hole.

The quasinormal spectrum of a stable black hole is an infinite set of complex frequencies which describes damped oscillations.

If there is at least one growing mode, the space−time is unstable
with the instability growth rate proportional to the imaginary part of the growing QNM.

Perturbative Stability of 4-dimensional blackholes

Konoplya and Zhidenko, RMP (2011) (arXiv:1102.4014)

Schwarzschild (M)	√
R−N (M, Q)	√
Schwarzschild−dS (M, $\Lambda > 0$)	√
Schwarzschild−AdS (M, $\Lambda < 0$)	√
R−N−dS (M, Q, Λ)	√
Kerr (M, J)	√
Kerr−dS (M, J, $\Lambda > 0$)	√
Kerr−AdS (M, J, $\Lambda < 0$)	√
Kerr−Newmann (M, J, Q)	?
Kerr−Newman−A(dS) (M, J, Q, Λ)	?
dilaton (M, Q, ϕ)	√
dilaton−axion (M, Q, J, ϕ , ψ)	?
dilaton−GB (M, ϕ)	√
Born−Infeld (M, Q)	√ (axial)
blackuniverses (M, ϕ)	√
BHs in the C−S theory (M, β)	unstable (*)

Most of the 4−dim. black holes proved to be stable.

Extreme Kerr & RN BHs are unstable.

Kerr−Newman BHs, and their string theory generalizations, which include axion and dilaton fields, are still ~~not tested~~ for stability.

(See Carlos Herdeiro's talk)

(*) if the coupling of the scalar field β is small enough.

Q : How about nonperturbative stability?

Higher ($D \geq 5$) dim BH & Gravitational instabilities

- A wide class of objects :
  black strings, black branes, black ring, saturn, etc.

- There exists various instabilities
  (non) Gregory-Laflamme instabilities

The qualitative phase diagram for the black objects in D ≥ 6

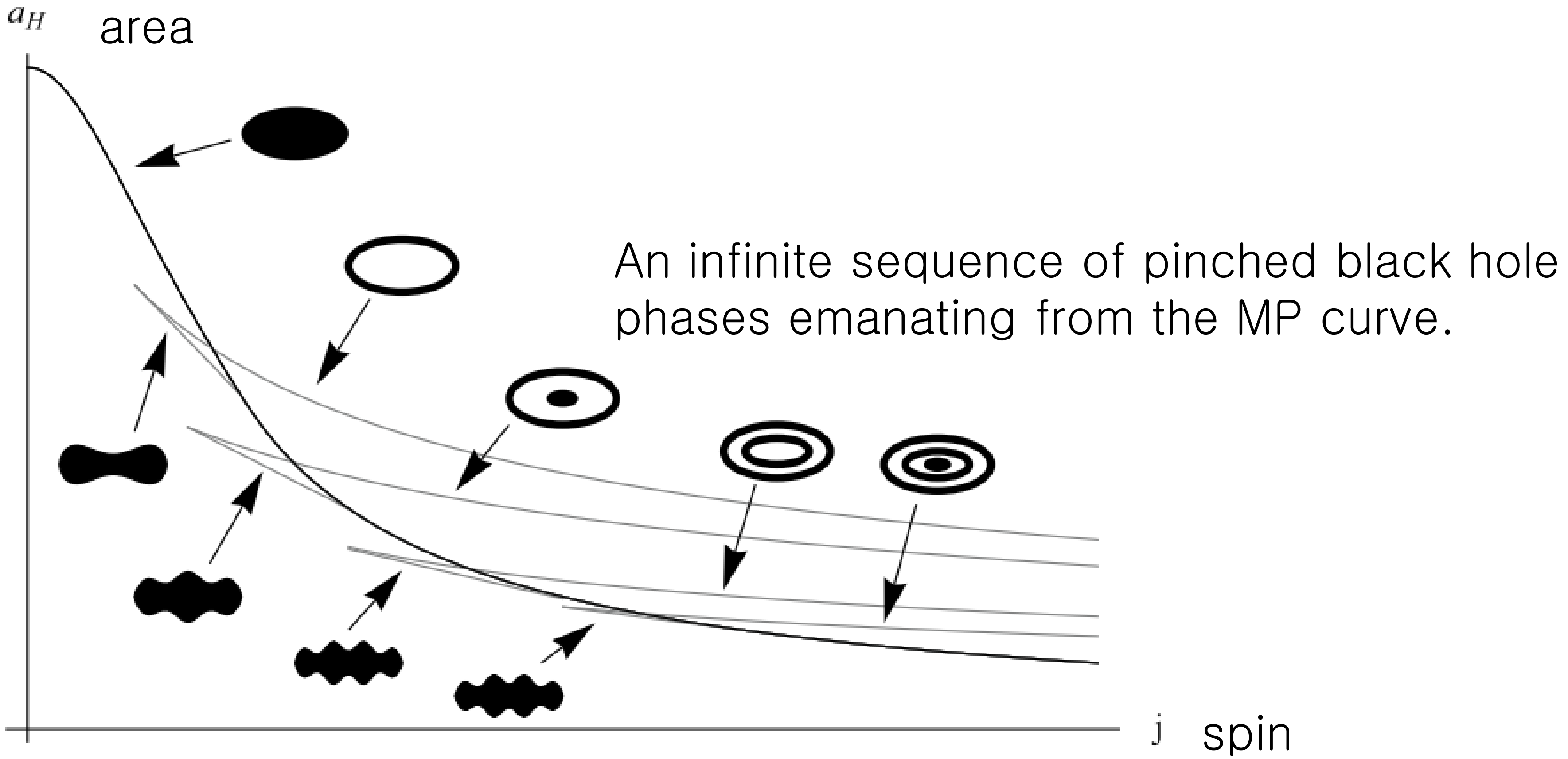

If thermal equilibrium is not imposed, multi-rings are possible in the upper region of the diagram.

(In)stability of higher-dimensional blackholes

Konoplya and Zhidenko, RMP (2011)

(arXiv:1102.4014)

Schwarzschild (M)	stable for all D
R-N (M, Q)	stable for D =5,6,⋯,11 & non-extremal charge
Schwarzschild-dS (M, Λ),	stable for D =5, 6, . . . 11
Schwarzschild-AdS (M, Λ)	stable in EM theory for D =5, 6, . . .
RN-dS (M, Q, $\Lambda > 0$)	unstable for D =7, 8, . . . 11
RN-AdS (M, Q, $\Lambda < 0$)	stable in EM theory and unstable in SUGRA 5
Gauss-Bonnet (M, α)	unstable for moderate and large α
Myers-Perry & generalizations (M, J)	? only particular types of perturbations
dilaton (M, Q, ϕ)	?
dilaton-axion (M, Q, J, ϕ , ψ)	?
dilaton-GB (M, ϕ , α)	?

NonperturbativeBlack Hole Stability

Fragmentation instability

is based on the entropy preference between the solutions.

Emparan and Myers, JHEP 0309, 025 (2003).

Apply thermodynamic 2nd law to initial (one black hole) and final(fragmented two black holes) phase.

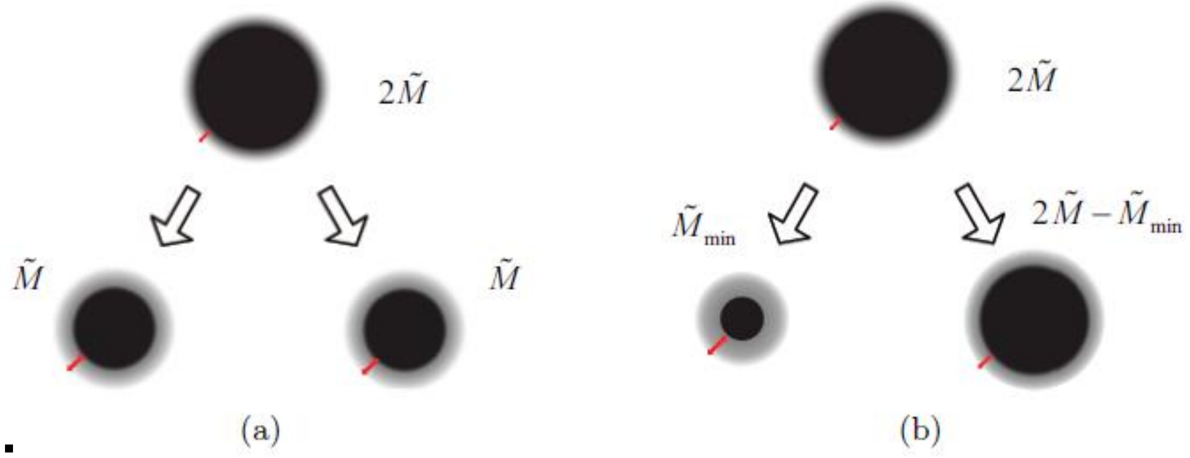

entropy of 1 BH < entropy of 2 fragmented BHs

$\longrightarrow$ (transition to) instability

Myers-Perry blackhole : Rotating Black hole in higher dimensions
There doesn't exist any upper limit on the angular momentum

Myers-Perry blackhole becomes unstable for large angular momentum into fragmentation.

RN blackhole is also thermodynamically unstable in specific parameter region.

Rotating AdS black hole and charged AdS black hole show the fragmentation instability in some parameter range

Fragmentation allows the upper or lower bound of black hole charges.

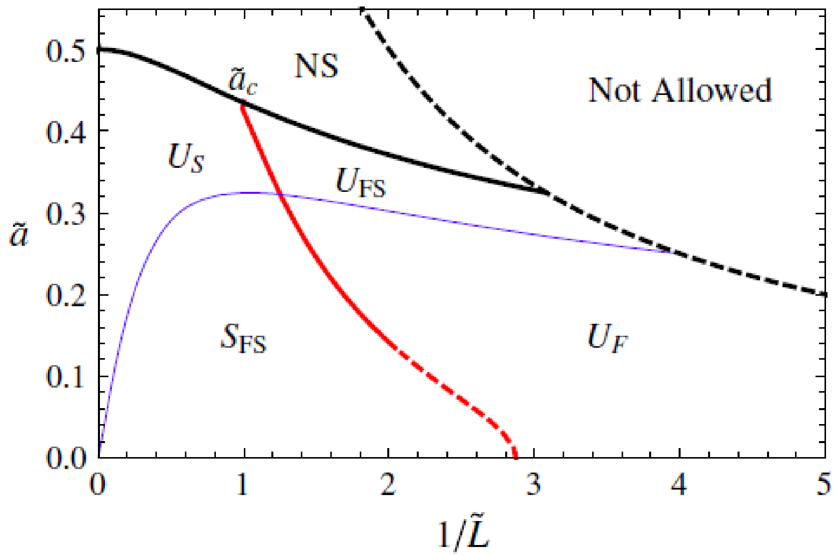

B. Gwak and BHL, PRD91 (2015) 6, 064020.

B.Gwak, BHL, D. Rho, Phys.Lett. B761 (2016)

S_{FS} stable under both fragmentation and superradiance.
U_F unstable under fragmentation.
U_S unstable under superradiance.
U_{FS} unstable under both fragmentation and superradiance.

This final phase is specified by a mass ratio $\delta = \frac{\tilde{m}}{\tilde{M}}$. We denote final phase as $(\delta, 1-\delta)$. $\bar{\delta} \leq \delta \leq$ ½ $\bar{\delta}$ minimum mass ratio given as $\bar{\delta} = \frac{\tilde{M}_{min}}{\tilde{M}}$. The minimum mass ratio has a finite value in DGB black hole, because the black hole has minimum mass $\tilde{M}_{min}$. The black holes can be fragmented only when it exceeds twice of minimum mass. With a black hole mass below twice of minimum mass, there are no fragmented black hole solutions, so these black holes are absolutely stable.

The mass and momenta of the black hole are related

$$\tilde{M} = \sqrt{(\delta\tilde{M})^2 + P_1^2} + \sqrt{(1-\delta)^2\tilde{M}^2 + P_2^2}\,. \qquad (21)$$

The linear momenta are arbitrary, so we set $P_1 = P_2 = 0$ to maximize the total entropy of the final phase. In this condition, the black hole slightly breaks into two black holes with negligible momenta. The initial phase decays to the final phase if the entropy is larger than that of the initial phase.

For Schwarzschild black hole

$$\frac{S_f}{S_i} = \frac{(\delta\,\tilde{r}_h)^2 + ((1-\delta)\,\tilde{r}_h)^2}{\tilde{r}_h^2} = \delta^2 + (1-\delta)^2\,, \tag{22}$$

The entropy ratio is always smaller than 1.
Therefore, a Schwarzschild black hole is always stable under fragmentation.
The entropy ratio marginally approaches 1 in
$\delta \to 0,$

These phenomena become different in the theory with the higher order of curvature term.

The EGB black hole solution is the same as the Schwarzschild one. However, the GB term contributes to the black hole entropy and influence stability.

For a black hole in EGB theory

The initial black hole entropy is

$$S_i = \frac{A_H}{4G}\left(1 + \frac{8\alpha\kappa}{\tilde{r}_h^2}\right) = \frac{\pi}{G}\left(\tilde{r}_h^2 + 8\alpha\kappa\right) . \tag{24}$$

Unlike Schwarzschild black holes, the fragmentation instability occurs depending on the fragmentation ratio δ. For the case of $(\delta, 1-\delta)$ fragmentation, the final phase entropy is given

$$S_f = \frac{\pi}{G}\left((\delta\tilde{r}_h)^2 + 8\alpha\kappa\right) + \frac{\pi}{G}\left(((1-\delta)\tilde{r}_h)^2 + 8\alpha\kappa\right) . \tag{25}$$

The EGB black hole is unstable if,

$$\frac{S_f}{S_i} = \frac{\left((\delta\tilde{r}_h)^2 + 8\alpha\kappa\right) + \left(((1-\delta)\tilde{r}_h)^2 + 8\alpha\kappa\right)}{\left(\tilde{r}_h^2 + 8\alpha\kappa\right)} > 1 . \tag{26}$$

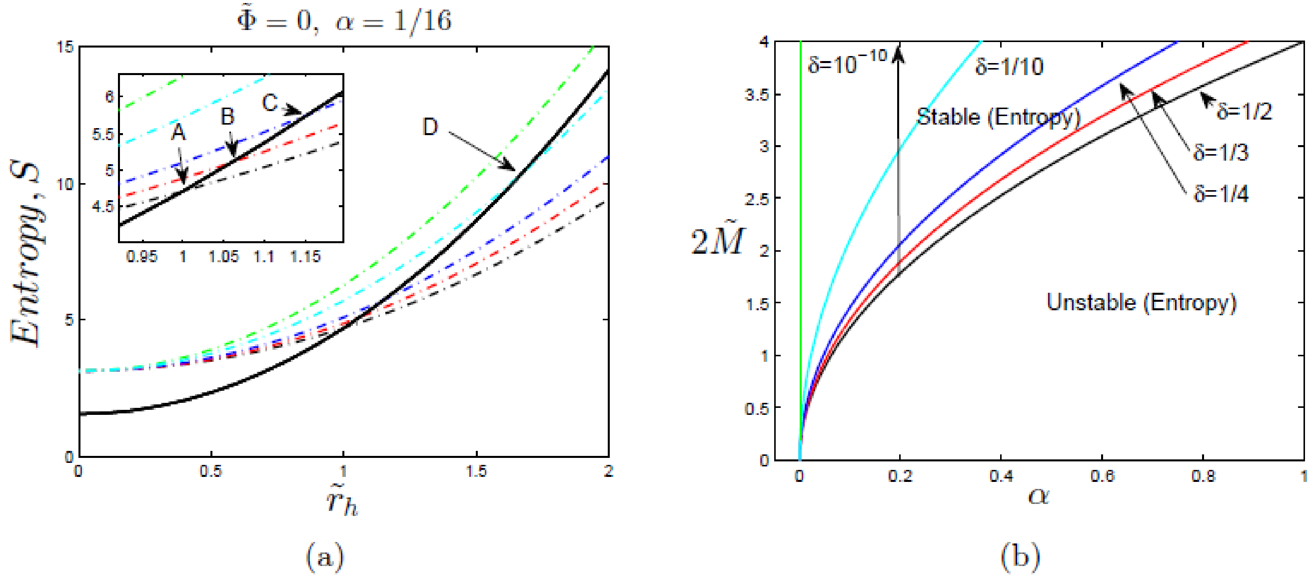

Figure 4: (a) Fragmentation ratio and EGB black hole entropy. The black solid line is initial phase entropy. The black, red, blue, cyan, and green dashed-dot lines are cases of $(\frac{1}{2},\frac{1}{2})$, $(\frac{1}{3},\frac{2}{3})$, $(\frac{1}{4},\frac{3}{4})$, $(\frac{1}{10},\frac{9}{10})$, and $(10^{-10}, 1-10^{-10})$. The crossing points go up from point A to D with changing δ. We fix κ=1. (b) Phase diagram of EGB black hole for δ=1/2 (black solid line), δ=1/3 (red solid line), δ=1/4 (blue solid line), δ=1/10 (cyan solid line) and δ=10^{-10} (green solid line) fragments corresponding to crossing points between initial and final phase of the black hole entropy in each color of line same to those in figure (a).

The mass ratio can have continuous values, and the black hole has stable and unstable phases. The minimum unstable region is at $\delta = \frac{1}{2}$. For the limit of $\delta \to 0$, all of EGB black holes become unstable for fragmentation as shown in 4(b).

For a black hole in DGB theory

The DGB black hole has a GB term coupled with a scalar field, so additional entropy correction comes from the higher curvature term. The DGB black hole entropy is

$$S = \frac{\pi \tilde{r}_h^2}{G}\left(1 + \frac{8\alpha\kappa}{\tilde{r}_h^2} e^{-\gamma\tilde{\Phi}_h}\right), \tag{28}$$

where a EGB black hole case corresponds to $\gamma = 0$ **. The DGB black hole entropy ratio between the initial and the final entropy including the higher-curvature corrections**

$$\frac{S_f}{S_i} = \frac{\left((\delta\tilde{r}_h)^2 + 8\alpha\kappa e^{-\gamma\tilde{\Phi}_\delta}\right) + \left(((1-\delta)\tilde{r}_h)^2 + 8\alpha\kappa e^{-\gamma\tilde{\Phi}_{1-\delta}}\right)}{\left(\tilde{r}_h^2 + 8\alpha\kappa e^{-\gamma\tilde{\Phi}_h}\right)}, \tag{29}$$

In the large mass limit $\tilde{r}_h \gg 1$, the entropy ratio becomes that of Schwarschild case,

$$\frac{S_f}{S_i} = \delta^2 + (1-\delta)^2 < 1. \tag{30}$$

Thus, massive DGB black holes are stable under fragmentation. The small mass limits are bounded to $\tilde{M}_{min}$. DGB black holes of mass $\tilde{M}_{min}$ are absolutely stable, because there are no fragmented black hole solutions. Larger than $\tilde{M}_{min}$, the black hole stability is dependent on an entropy correction term. The entropy ratio is given

$$\frac{S_f}{S_i} = \frac{\delta^2 + (\delta-1)^2 + \frac{8\alpha\kappa e^{-\gamma\bar{\Phi}_\delta} + 8\alpha\kappa e^{-\gamma\bar{\Phi}_{1-\delta}}}{\tilde{r}_h^2}}{1 + \frac{8\alpha\kappa e^{-\gamma\bar{\Phi}_h}}{\tilde{r}_h^2}}, \tag{31}$$

where the horizon radius square term is important in the small black hole. The entropy ratio may increase in smaller mass like EGB black holes, but there is ambiguity since DGB black holes have a minimum mass. In this part, there is no proper approximation to describe the instabilities of small mass DGB black holes. It should be pointed out through numerical calculation. Also, the minimum mass bounds the fragmentation mass ratio. It is not seen in the Schwarzschild black hole or EGB black hole. The DGB black holes have more variety properties and behaviors. We will obtain detailed behaviors through the numerical calculation.

Fragmentation Instability for DGB Black Holes

We investigate the fragmentation instability using a numerical analysis.

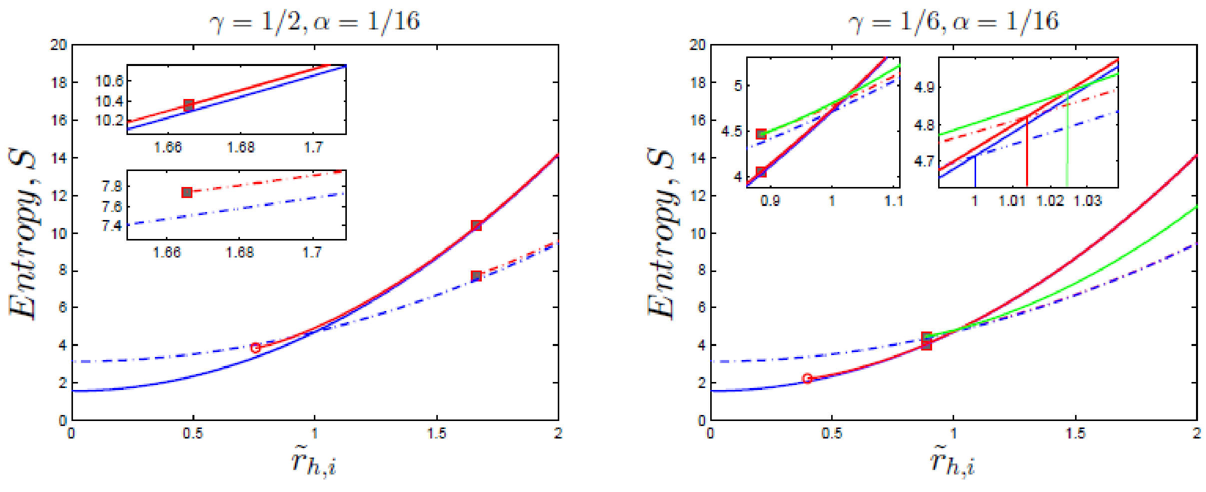

(a) (b)

Figure 6: The initial and final phase entropies with respect to $r_{h,i}$ for given couplings γ and α. The blue solid line and blue dashed-dot line are initial and final phase entropies in EGB theory as a reference for $(\frac{1}{2}, \frac{1}{2})$. The red solid line and red dashed-dot line are initial and final phase entropies in DGB theory for $(\frac{1}{2}, \frac{1}{2})$. Initial phase exists above red circle for minimum mass. Final phase exists above red box for $(\frac{1}{2}, \frac{1}{2})$. The green solid line represents fragmentation for marginal mass ratio $\bar{\delta}$.

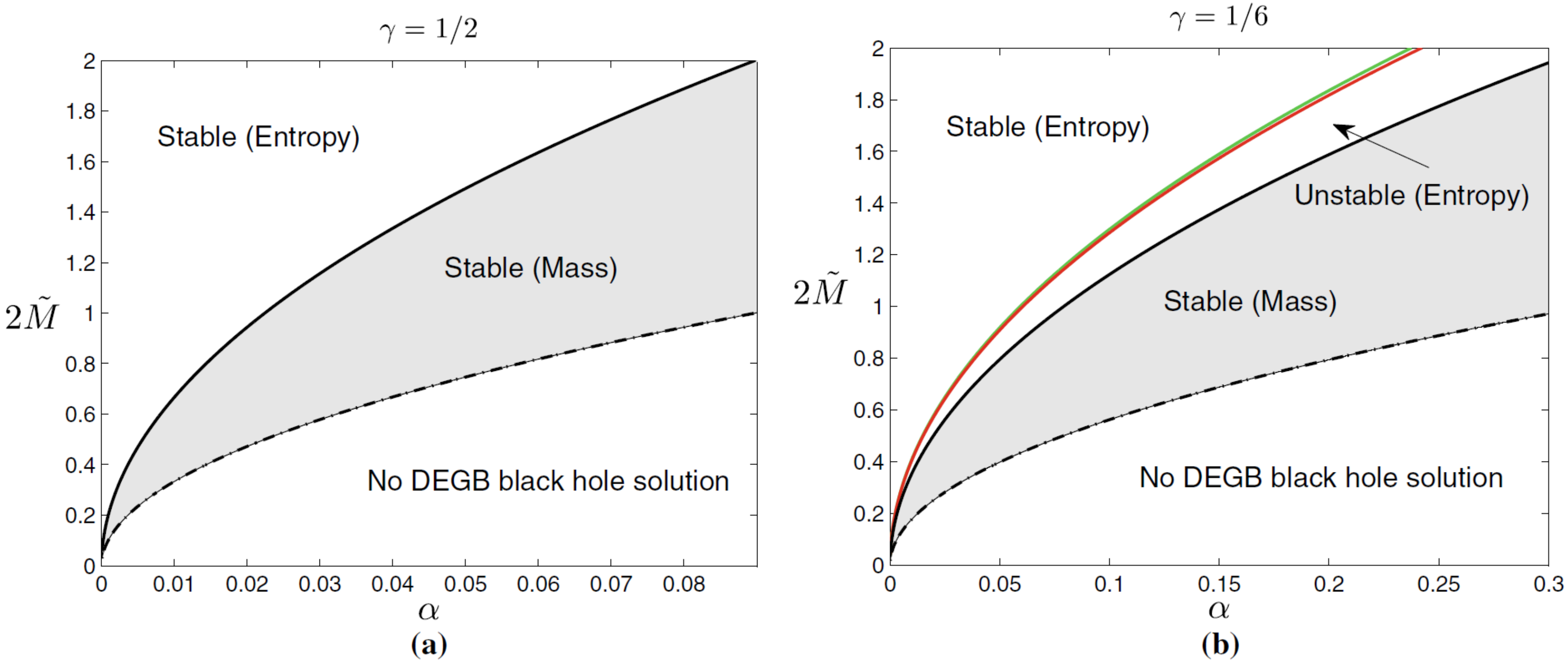

The phase diagrams with respect to α and $\tilde{M}$ in fixed γ .
The red solid line represents (1/2 ,1/2) fragmentation.
The green solid line represent $(\bar{\delta}, 1-\bar{\delta})$ fragmentation

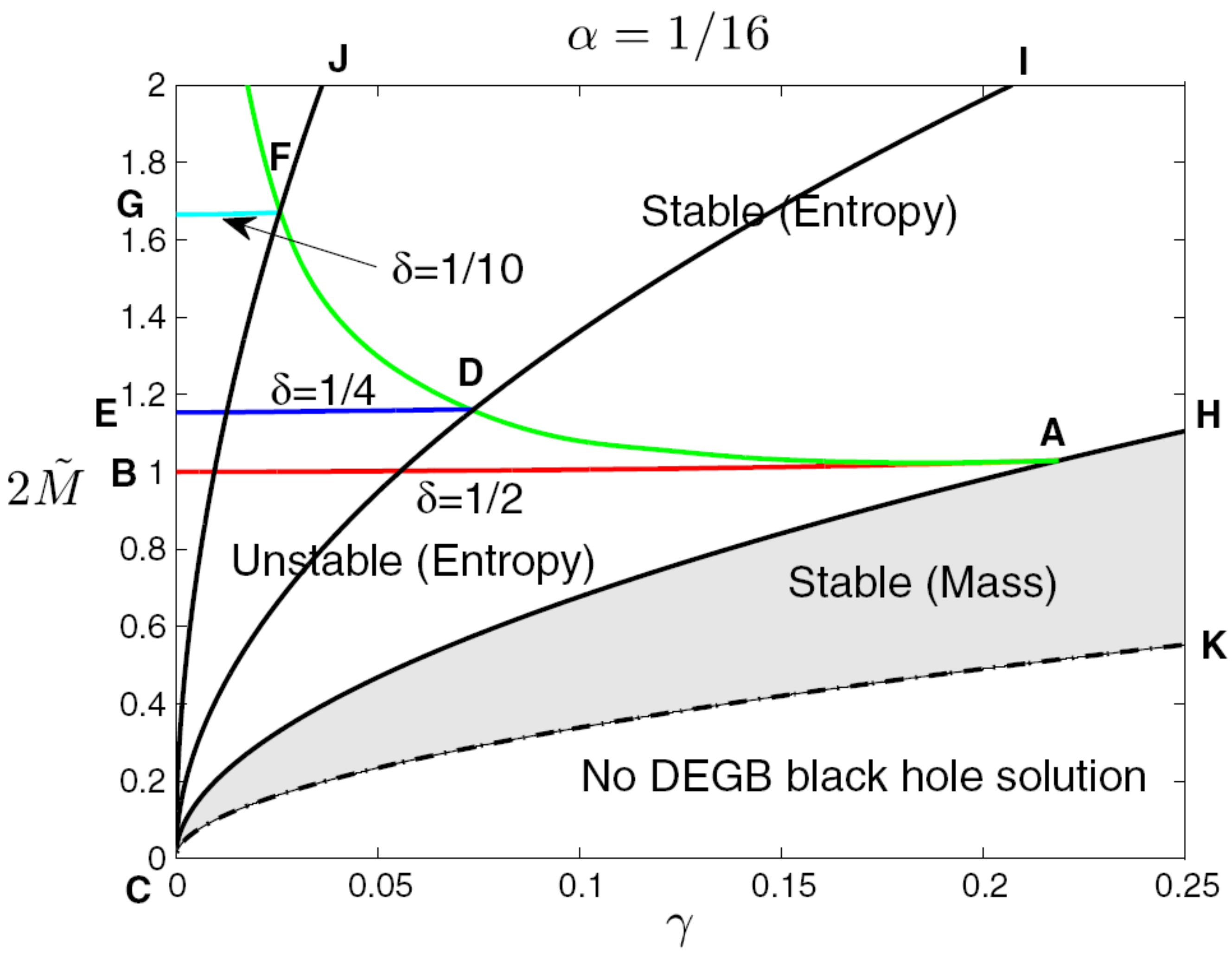

The phase diagrams with respect to γ and $\widetilde{M}$ for fixed α for (1/2 ,1/2) (red solid line), (1/4 , 3/4) (blue solid line), (1/10 , 9/10) (cyan solid line), and $(\bar{\delta}, 1-\bar{\delta})$ (green solid line) fragmentation

3.Cosmological Effects of the Gauss-Bonnet term – Inflation

- An action with a Gauss-Bonnet term:

$$S = \int d^4x \sqrt{-g}\left[\frac{1}{2\kappa^2} R - \frac{1}{2} g^{\mu\nu}\partial_\mu\phi\partial_\nu\phi - V(\phi) - \frac{1}{2}\xi(\phi)R_{GB}^2\right]$$

Gauss-Bonnet term
$R_{GB}^2 = R_{\mu\nu\rho\sigma}R^{\mu\nu\rho\sigma} - 4R_{\mu\nu}R^{\mu\nu} + R^2$

$$G_{\mu\nu}=\kappa^2\left(T_{\mu\nu} + T_{\mu\nu}^{GB}\right)$$

$$T_{\mu\nu} = \partial_\mu\phi\partial_\nu\phi + V(\phi) - \frac{1}{2}g_{\mu\nu}\left(g^{\rho\sigma}\partial_\rho\phi\partial_\sigma\phi + 2V\right)$$

$\kappa^2 = 8\pi G$ $\quad G_{\mu\nu} \equiv R_{\mu\nu} - \frac{1}{2} g_{\mu\nu} R$

$$T_{\mu\nu}^{GB} = 4\left(\partial^\rho\partial^\sigma\xi R_{\mu\rho\nu\sigma} - \Box\xi R_{\mu\nu} + 2\partial_\rho\partial_{(\mu}\xi R_{\nu)}^{\rho} - \frac{1}{2}\partial_\mu\partial_\nu\xi R\right) - 2\left(2\partial_\rho\partial_\sigma\xi R^{\rho\sigma} - \Box\xi R\right)g_{\mu\nu}$$

$$\Box\phi - V_{,\phi}(\phi) - \frac{1}{2}T^{GB} = 0 \qquad T^{GB} = \xi_{,\phi}(\phi)R_{GB}^2$$

- FLRW Universe metric: $ds^2 = -dt^2 + a^2(t)\left(\frac{dr^2}{1-Kr^2} + r^2(d\theta^2 + \sin^2\theta\, d\varphi^2)\right)$

Einstein and Field equations yield:

$$H^2 = \frac{\kappa^2}{3}\left(\frac{1}{2}\dot\phi^2 + V - \frac{3K}{\kappa^2 a^2} + 12\dot\xi H\left(H^2 + \frac{K}{a^2}\right)\right)$$

$$\dot H = -\frac{\kappa^2}{2}\left(\dot\phi^2 - \frac{2K}{\kappa^2 a^2} - 4\ddot\xi\left(H^2 + \frac{K}{a^2}\right) - 4\dot\xi H\left(2\dot H - H^2 - \frac{3K}{a^2}\right)\right)$$

$$\ddot\phi + 3H\dot\phi + V_{,\phi} + 12\xi_{,\phi}\left(H^2 + \frac{K}{a^2}\right)\left(\dot H + H^2\right) = 0$$

Inflation with a Gauss–Bonnet

- Action $$S = \int d^4x \sqrt{-g}\left[\frac{1}{2\kappa^2} R - \frac{1}{2} g^{\mu\nu}\partial_\mu\phi\partial_\nu\phi - V(\phi) - \frac{1}{2}\xi(\phi)R^2_{GB}\right]$$

Einstein and Field equations yield:

$$H^2 = \frac{\kappa^2}{3}\left(\frac{1}{2}\dot{\phi}^2 + V - \frac{3K}{\kappa^2 a^2} + 12\dot{\xi}H\left(H^2 + \frac{K}{a^2}\right)\right)$$

$$\dot{H} = -\frac{\kappa^2}{2}\left(\dot{\phi}^2 - \frac{2K}{\kappa^2 a^2} - 4\ddot{\xi}\left(H^2 + \frac{K}{a^2}\right) - 4\dot{\xi}H\left(2\dot{H} - H^2 - \frac{3K}{a^2}\right)\right)$$

$$\ddot{\phi} + 3H\dot{\phi} + V_{,\phi} + 12\xi_{,\phi}\left(H^2 + \frac{K}{a^2}\right)\left(\dot{H} + H^2\right) = 0$$

S. Koh, BHL, W. Lee, Tumurtushaa
PRD90 (2014) no.6, 063527

S. Koh, BHL, W. Lee, Tumurtushaa
arXiv:1610.04360

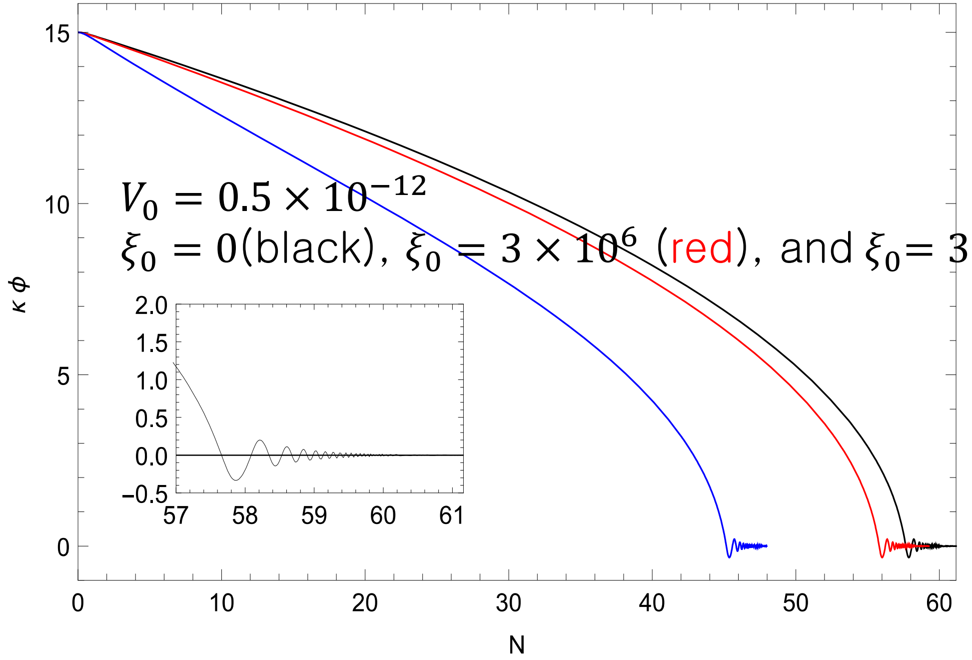

$V_0 = 0.5 \times 10^{-12}$
$\xi_0 = 0$(black), $\xi_0 = 3 \times 10^6$ (red), and $\xi_0 = 3 \times 10^7$ (blue).

The duration of inflation gets shorter as the Gauss–Bonnet coupling constant increases.
(making the effective potential steeper)

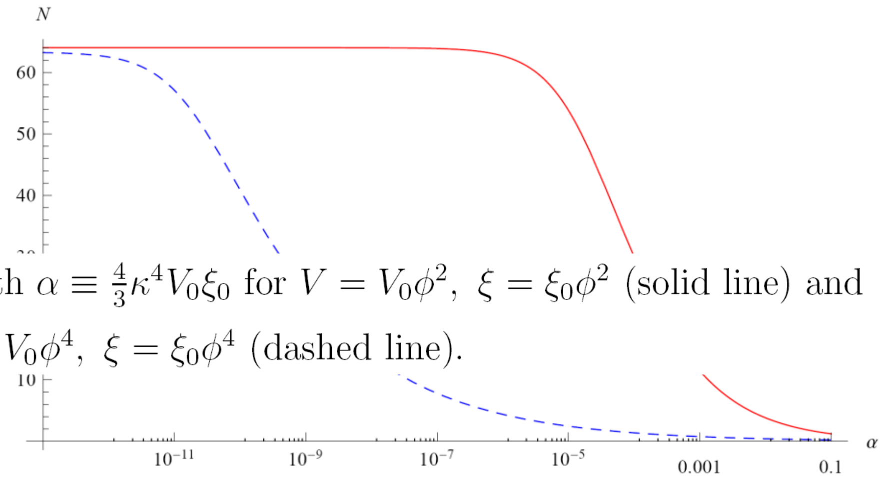

e-folding numbers with $\alpha \equiv \frac{4}{3}\kappa^4 V_0\xi_0$ for $V = V_0\phi^2$, $\xi = \xi_0\phi^2$ (solid line) and $V = V_0\phi^4$, $\xi = \xi_0\phi^4$ (dashed line).

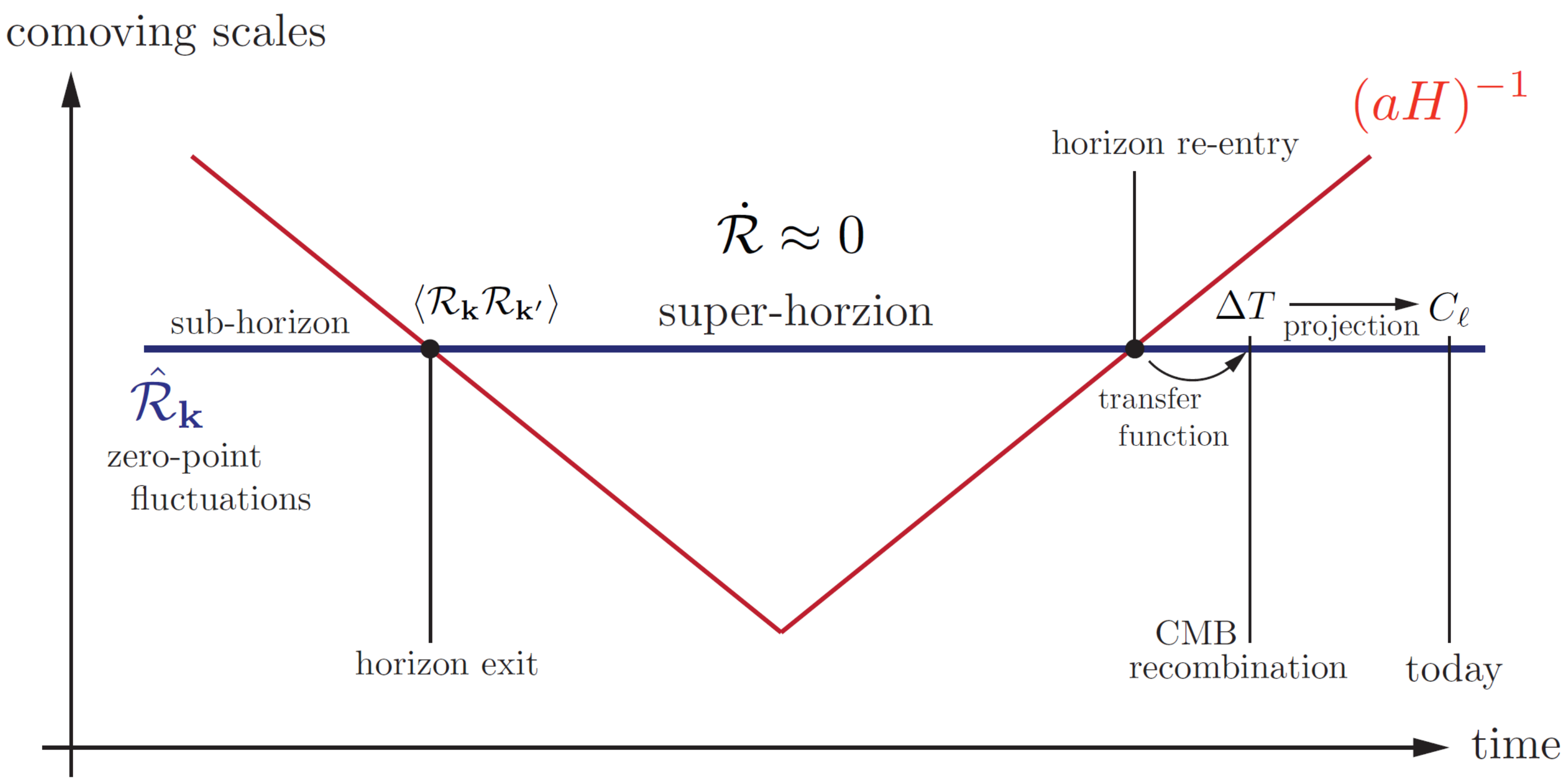

comoving scales
$(aH)^{-1}$
horizon re-entry
$\dot{\mathcal{R}} \approx 0$
$\langle \mathcal{R}_{\mathbf{k}} \mathcal{R}_{\mathbf{k}'} \rangle$
sub-horizon
super-horzion
ΔT
projection
C_ℓ
$\hat{\mathcal{R}}_{\mathbf{k}}$
zero-point
fluctuations
transfer
function
horizon exit
CMB
recombination
today
time

Model-2

$$V(\phi) = V_0\phi^n, \quad \xi(\phi) = \xi_0\phi^n$$

The number of e-folds before the end of inflation

$$N(\phi) \simeq \int_{\phi_e}^{\phi} \frac{\kappa^2}{Q} d\phi \simeq \frac{\kappa^2\phi^2}{2n}\, {}_2F_1\left(1; \frac{1}{n}; 1+\frac{1}{n}; -\alpha\phi^{2n}\right)$$

$$\phi \simeq \sqrt{\frac{2nN}{\kappa^2}}\left[1 + \frac{\alpha(2nN)^n}{2(n+1)\kappa^{2n}}\right]$$

$$n_s - 1 \simeq -\frac{n+2}{2N} + \frac{n(3n+2)(2nN)^n\alpha}{2(1+n)N\kappa^{2n}},$$

$$n_t \simeq -\frac{n}{2N} - \frac{n^2(2nN)^n\alpha}{2(1+n)N\kappa^{2n}},$$

$$r \simeq \frac{4n}{N} + \frac{4n(2n+1)(2nN)^n\alpha}{(1+n)N\kappa^{2n}},$$

$$\frac{dn_s}{d\ln k} \simeq -\frac{n+2}{2N^2} - \frac{n(n-1)(3n+2)(2nN)^n\alpha}{2(1+n)N^2\kappa^{2n}},$$

$$\frac{dn_t}{d\ln k} \simeq -\frac{n}{2N^2} + \frac{n^2(n-1)(2nN)^n\alpha}{2(1+n)N^2\kappa^{2n}}$$

➢ Model-2

$$V(\phi) = V_0\phi^n, \quad \xi(\phi) = \xi_0\phi^n$$

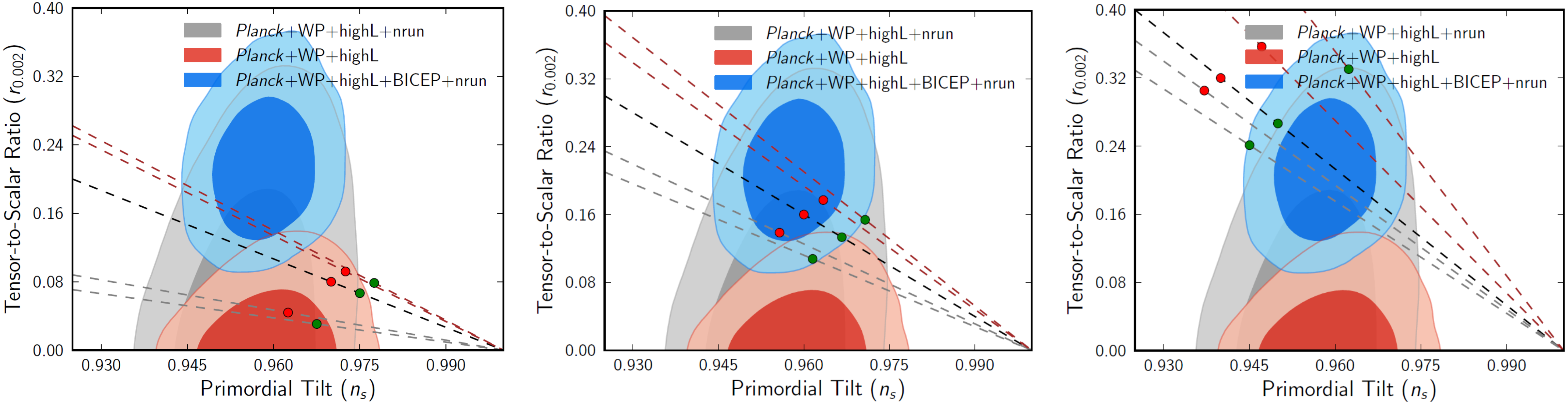

TABLE I: Observationally favored range of model parameter α for different values of n and N from observational data set.

Model n	Parameter range for N=50	Parameter range for N=60
n=1	$-6.6\times10^{-3}\leq\alpha\leq2\times10^{-3}$	$-5.5\times10^{-3}\leq\alpha\leq4\times10^{-4}$
n=2	$-5.2\times10^{-6}\leq\alpha\leq6\times10^{-6}$	$-3.2\times10^{-6}\leq\alpha\leq1.5\times10^{-6}$
n=4	lies outside of 2σ boundary	$0\leq\alpha\leq2.5\times10^{-12}$

➢ Model-2

$$V(\phi) = V_0\phi^n, \quad \xi(\phi) = \xi_0\phi^n$$

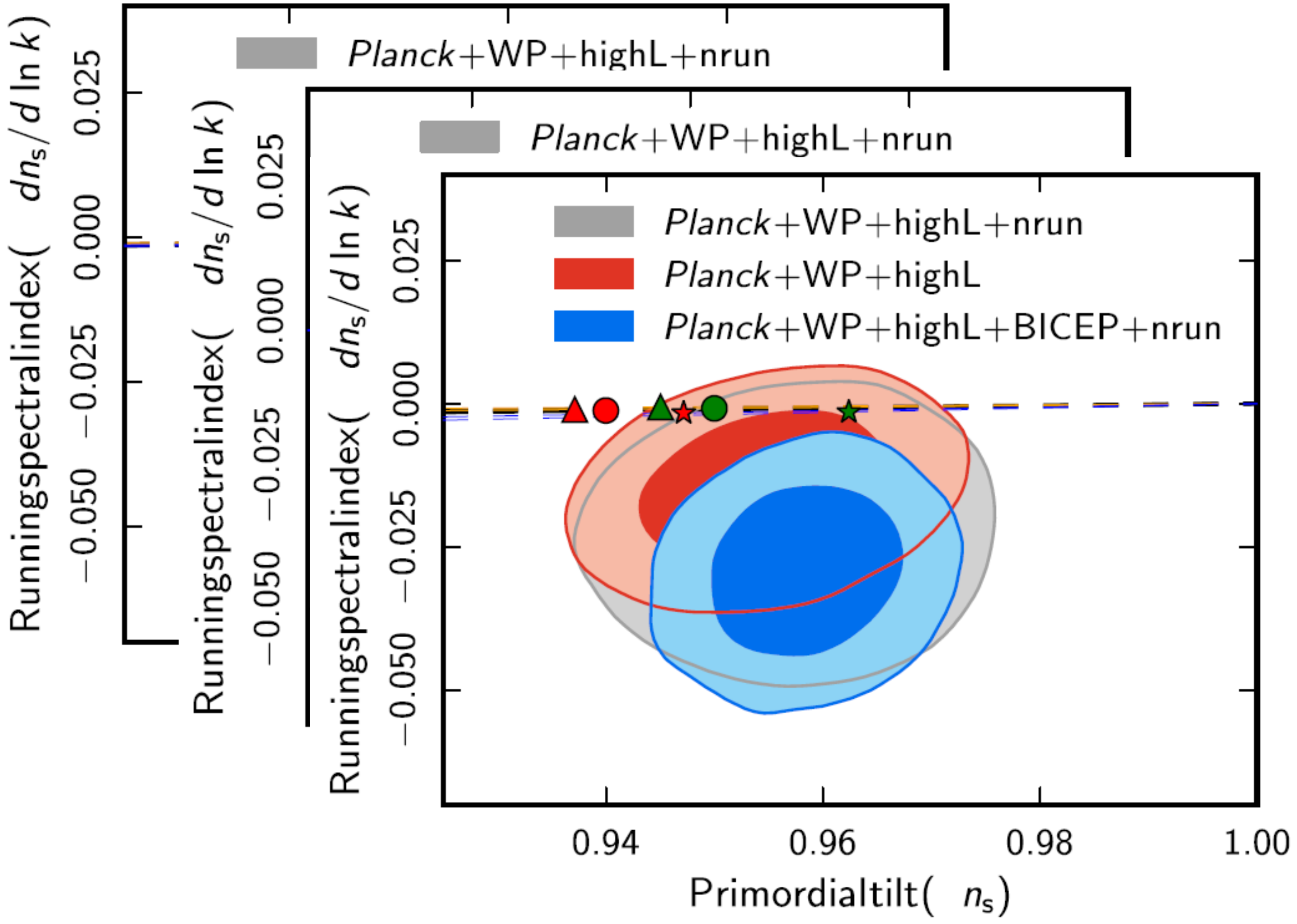

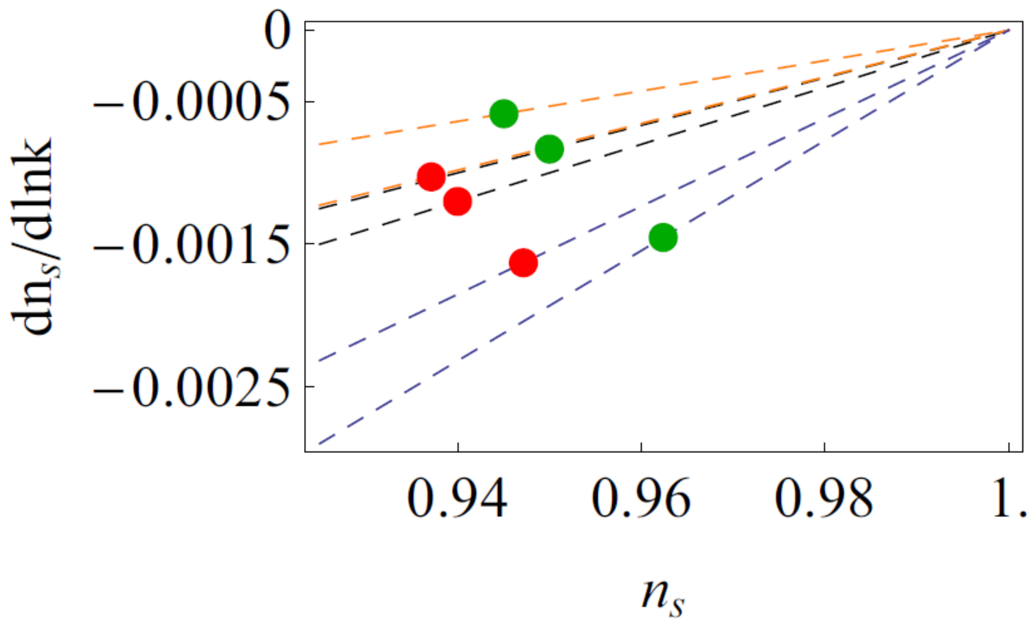

Reheating parameters in Gauss-Bonnet inflation Models

Let us consider a mode with comoving wavenumber k_* which crosses the horizon during inflation when the scale factor is a_*. The comoving Hubble scale $a_* H_* = k_*$ at the horizon crossing time can be related to that of the present time as

$$\frac{k_*}{a_0 H_0} = \frac{a_*}{a_{\rm end}} \frac{a_{\rm end}}{a_{\rm th}} \frac{a_{\rm th}}{a_0} \frac{H_*}{H_0}\,, \tag{6}$$

where a_0, a_*, $a_{\rm end}$, and $a_{\rm th}$ denote the scale factor at present, the horizon crossing, the end of inflation, and the end of reheating, respectively. By taking logarithm from both sides, we rewrite

$$\ln \frac{k_*}{a_0 H_0} = -N_* - N_{\rm th} + \ln \frac{a_{\rm th}}{a_0} + \ln \frac{H_*}{H_0}\,, \tag{7}$$

where $N_* \equiv \ln(a_{\rm end}/a_*)$ is the number of e-foldings between the time of mode exits the horizon and the end of inflation, and $N_{\rm th} \equiv \ln(a_{\rm th}/a_{\rm end})$ is the number of e-foldings between the end of inflation and the end of reheating.

4.Summary

We have studied the Black Hole with Gauss-Bonnet term

- Numerically constructed the static DGB **hairy** black hole in asymptotically flat spacetime

  There exists **minimum mass**, etc. ("repulsive" gravity effect)

- **Fragmentation instability of black holes:**

  When the scalar field on the horizon is the maximum, the DGB black hole solution has the minimum horizon size.

  The amount of black hole hair decreases as the DGB black hole mass increases. DGB black hole configurations go to EGB black hole cases for small α and γ.

  The DGB black hole phase is unstable under fragmentation, even if these phases are stable under perturbation.

  We have found the phase diagram of the fragmentation instability for a black hole mass and two couplings.

Summary - continued

We have reviewed the stability of black holes.
4 dim. and higher dim.
perturbative and nonperturbative (fragmentation)

Most of the 4-dim. black holes are perturbatively stable.
(Stability of Kerr-Newman blackholes, & generalizations including axion and dilaton fields, are still not clear.

Higher Dim. BH : rich phases,
(non)Gregory-Laflamme instabilities

For rotating AdS BH, the instability sources are
: Kerr bound.
: superradiance instability,
: BPS-like $a = |l|$ bound.
There exists region
unstable under fragmention while perturbatively stable.

GB term in inflation

- We have investigated the slow-roll inflation with the GB term which coupled to the inflaton field nonminimally. We have considered the potential and coupling functions as

$$V(\phi) = V_0 e^{-\lambda\phi}, \quad \xi(\phi) = \xi_0 e^{-\lambda\phi} \qquad V(\phi) = V_0 \phi^n, \quad \xi(\phi) = \xi_0 \phi^n$$

- First, we have applied our general formalism to the large-field inflationary model with exponential potential and exponential coupling. In this case, we could find the valid model parameter range for inflation to happen, unfortunately, these parameter ranges are not favored by the data sets.

- Second, we have studied models with monomial potential and monomial coupling to GB term. In this case, r is enhanced for $\alpha > 0$ while it is suppressed for $\alpha < 0$.

- GB term makes the e-folding smaller.

- N≈60 condition requires that $\alpha \approx 10^{-6}$ for V$\sim\varphi^2$ $\alpha \approx 10^{-12}$ for V$\sim\varphi^4$.

- In this work, running spectral index turns out to be inconsistent with BICEP2+Planck data. It would be interesting to search for the alternatives to reconcile Planck data with BICEP2 besides consideration of the running spectral index.

The model parameter must take values in interval between $2.1276 \times 10^6 \leq \xi_0 \leq 3.7796 \times 10^6$ to be consistent with accuracy of future observation in which $n_s = 0.9682 \pm 10^3$.

Other Effects such as the reheating under investigation

Thank You!